Norman, J. A., Drummond, A. H., & Moser, P. (1979) *Mol. Pharmacol. 16*, 1089–1094.
Potter, J. C., & Gergely, J. (1975) *J. Biol. Chem. 250*, 4628–4633.
Reid, R. E., Gariépy, J., Saund, A. K., & Hodges, R. H. (1981) *J. Biol. Chem. 256*, 2742–2751.
Roufogalis, B. D. (1981) *Biochem. Biophys. Res. Commun. 98*, 607–613.
Sellinger-Barnette, M., & Weiss, B. (1982) *Mol. Pharmacol. 21*, 86–91.
Walsh, M., Stevens, F. C., Oikawa, K., & Kay, C. M. (1978) *Biochemistry 17*, 3924–3930.
Wang, C.-L. A., Aquaron, R. R., Leavis, P. C., & Gergely, J. (1982) *Eur. J. Biochem. 124*, 7–12.
Weeks, R. A., & Perry, S. V. (1978) *Biochem. J. 173*, 449–457.

Stopped-Flow Studies of Myelin Basic Protein Association with Phospholipid Vesicles and Subsequent Vesicle Aggregation†

Paul D. Lampe,‡ G. Jason Wei, and Gary L. Nelsestuen*

ABSTRACT: When mixed with vesicles containing acidic phospholipids, myelin basic protein causes vesicle aggregation. The kinetics of this vesicle cross-linking by myelin basic protein was investigated by using stopped-flow light scattering. The process was highly cooperative, requiring about 20 protein molecules per vesicle to produce a measurable aggregation rate and about 35 protein molecules per vesicle to produce the maximum rate. The maximum aggregation rate constant approached the theoretical vesicle–vesicle collisional rate constant. Vesicle aggregation was second order in vesicle concentration and was much slower than protein–vesicle interaction. The highest myelin basic protein concentration used here did not inhibit vesicle aggregation, indicating that vesicle cross-linking occurred through protein–protein interactions. In contrast, poly(L-lysine)-induced vesicle aggregation was easily inhibited by increasing peptide concentrations, indicating that it did cross-link vesicles as a peptide monomer. The myelin basic protein:vesicle stoichiometry required for aggregation and the low affinity for protein dimerization suggested that multiple protein cross-links were needed to form a stable aggregate. Stopped-flow fluorescence was used to estimate the kinetics of myelin basic protein–vesicle binding. The half-times obtained suggested a rate constant that approached the theoretical protein–vesicle collisional rate constant.

Myelin protects and insulates selected nerve axons from the surrounding environment. Myelin membranes contain approximately 27% protein of which 31% is myelin basic protein (Rumsby & Crang, 1977). Myelin basic protein is rich in lysine and arginine residues and is believed to interact electrostatically with negatively charged phospholipids (Boggs & Moscarello, 1978a). Nonionic interactions have also been reported (Stollery et al., 1980; Boggs et al., 1981). Most evidence indicates that the protein is found only on the cytoplasmic side of myelin membranes (Peterson & Gruener, 1978; Golds & Braun, 1976; Poduslo & Braun, 1975).

One proposed role for myelin basic protein is maintenance of the multilaminar structure of the myelin sheath through membrane cross-linking. Chemical cross-linking of myelin basic protein in solution and in myelin indicated that the protein may span the intracellular space between adjacent lamellae as a dimer (Golds & Braun, 1978a,b). Self-association studies have also shown that myelin basic protein dimerizes in solution (Smith, 1980) and in the presence of detergent monomers (Smith, 1982). However, other work indicated that the protein was isolated as a monomer at high detergent concentrations and as a dimer at low detergent concentrations (Smith & McDonald, 1979). In addition, results of solubilization studies with the two fragments generated by BNPS-skatole[1] treatment of the protein led to the identification of the C terminal as the site for ionic interaction with lipids (Jones & Rumsby, 1977). These results were viewed as support for lamellae cross-linking as a protein monomer (Rumsby & Crang, 1977). Other studies indicated that both the N- and C-terminal peptides, generated by BNPS-skatole, interact with lipids (London et al., 1973; Boggs et al., 1981). Myelin basic protein was found to have a folded structure (Epand et al., 1974) which may be important in forming the membrane binding region.

Myelin basic protein has been reported to aggregate phospholipid vesicles (Smith, 1977a,b; Boggs & Moscarello, 1978b; Lampe & Nelsestuen, 1982). Aggregation of vesicles may constitute a model for cross-linking of myelin membranes. However, the turbid mixture that results from vesicle aggregation makes many simple physical measurements difficult. These problems can be minimized by analysis of changes immediately following mixing when the protein and vesicles are largely monomeric. The following study used stopped-flow fluorescence and light scattering techniques to study the association of myelin basic protein with phospholipid vesicles and the initial rates of vesicle aggregation. The kinetic parameters obtained can be used to calculate thermodynamic and stoi-

† From the Department of Biochemistry, University of Minnesota, St. Paul, Minnesota 55108. *Received October 12, 1982.* Supported in part by Grant HL 15728 from the National Institutes of Health. The quasi-elastic light scattering apparatus and stopped-flow were provided by the laboratory of Dr. Victor Bloomfield and are maintained by Grant PCM 8118107 from the National Science Foundation.

‡ To be submitted as part of a thesis by P.D.L. in partial fulfillment of the Ph.D. requirement, University of Minnesota.

[1] Abbreviations: PC, phosphatidylcholine; PG, phosphatidylglycerol; dansyl-PE, *N*-dansylphosphatidylethanolamine; HPLC, high-performance liquid chromatography; *n*, sample size; *r*, correlation coefficient; BNPS-skatole, 3-bromo-3-methyl-2-[(2-nitrophenyl)thio]indolenine.

0006-2960/83/0422-1594$01.50/0

chiometric ratios. When saturated with myelin basic protein, vesicle aggregation was rapid and approached the collisional rate. Kinetic analysis showed that vesicle aggregation was highly cooperative with respect to protein, indicating that multiple interactions were required for cross-linking. In addition, the results demonstrated that cross-linkling was due to protein–protein interaction, so the protein probably spans phospholipid membranes as a dimer.

Materials and Methods

PC was purchased from Avanti Polar Lipids, Inc., Birmingham, AL. PG and poly(L-lysine) (M_r 30000) were purchased from Sigma Chemical Co., St. Louis, MO. The phospholipids were reported to be greater than 98% pure. HPLC chromatography of the phospholipids (Hax et al., 1977) supported this high purity, and they were used without further purification. Dansyl-PE was prepared as previously described (Waggoner & Stryer, 1970) with the modifications of Pusey et al. (1982). Phospholipid concentrations were estimated by organic phosphate measurement (Chen et al., 1956). All of the phospholipid components in the vesicles are expressed in mole percentages.

Myelin basic protein was purified from bovine brains by the method of Eylar et al. (1974). An additional purification step consisted of gel filtration on a Sephadex G-75 superfine column (1.6 × 90 cm) to remove traces of contaminating protein. The final protein contained no contamination (<1% of the major protein band) as detected on polyacrylamide gel electrophoresis in sodium dodecyl sulfate using the method of Weber & Osborn (1969). The apparent molecular weight of 18000 corresponded to that of myelin basic protein. Protein was quantitated by using $E^{1\%}_{276.4} = 5.64$ (Liebes et al., 1975).

Phospholipid vesicles were prepared by the ethanol injection method of Kremer et al. (1977). Phospholipids were dissolved in 0.5 mL of ethanol and injected in 5-μL aliquots into a stirred 10.0-mL solution of buffer (0.1 M NaCl and 0.05 M Tris-HCl, pH 7.5) at room temperature. A standard method of injection was necessary to obtain vesicle populations of consistent size. PG/PC (30/70) vesicles obtained by this method had a diameter of 35 nm, a diffusion coefficient of 1.26×10^{-7} cm^2/s, a Stokes radius of 1.7×10^{-6} cm, and a molecular weight of 4.2×10^6. These values were determined by quasielastic light scattering analysis and light scattering intensity measurements using the apparatus and methods described elsewhere (Pletcher et al., 1980). Dialysis of the vesicles to remove ethanol appeared to have no effect on the vesicle aggregation studies, and the vesicles were usually used without dialysis.

Static fluorescence measurements were performed on a Hitachi Perkin-Elmer Model 44A fluorescence spectrometer. Stopped-flow light scattering measurements were carried out in an apparatus previously described (Wei et al., 1982). A 50-mW HeNe laser (Spectral Physics 125) was used as the light source, and the intensity was attenuated by neutral density filters as needed. The 90° scattered light from the optical cell of a Durrum D-130 mixing apparatus was collected by a lens-split assembly and measured by a RCA 7265 photomultiplier tube equipped with a PAR 114 amplifier. Stopped-flow fluoresence used the same apparatus except a 450-W xenon lamp was used as the light source (SLM Instruments), a 277-nm band-pass filter (LKB Instruments, Inc.) was placed in front of the sample cell, and a 410-nm cutoff filter (Corning, CS-3-73) was inserted in front of the photomultiplier. The output signals were recorded digitally in a Fabri-Tek 1010 transient recorder. To increase the signal to noise ratio, four curves were averaged when collecting stopped-flow fluorescence data. All of the protein and phospholipid concentrations are expressed after mixing in the stopped-flow apparatus. The dead time for this instrument was estimated to be 8 ms (Wei et al., 1982). The same buffer, 0.05 M Tris-HCl (pH 7.5)–0.1 M NaCl, was used throughout these experiments.

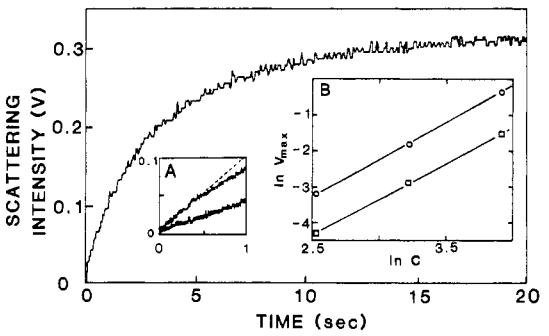

FIGURE 1: Chart tracing of the light scattering intensity when myelin basic protein and phospholipid vesicles were mixed. The final concentration of PG/PC (30/70) vesicles was 25 μg/mL and that of myelin protein was 10 μg/mL. Inset A: Upper curve is a chart tracing under the same conditions with the time scale expanded. The lower curve is a tracing obtained from a mixture of protein (4 μg/mL) and the above vesicles. Inset B: Double-logarithmic plot of maximum velocity (V/s) vs. concentration of phospholipid in the vesicles (μg/mL). Protein concentration was 40 μg/mL and vesicle composition ratios of PG/PC were (○) 30/70 and (□) 15/85. The lines drawn have a slope of 2.

The initial rate of reaction was used to estimate the rate constants. The initial rate, in most cases, should correspond to the dimerization of myelin basic protein coated vesicles. The rate constant is simply $k = (dI/dt)_{t=0}/(I_{t=0}C_{t=0})$, where I is the intensity of the scattered light which is proportional to the apparent molecular weight, C is the molar concentration of the vesicles, and t is the time after mixing. Linear increases in light scattering intensity usually extended well beyond the level expected for a vesicle dimer. As the particle size increases, the corresponding diffusion coefficient decreases. Over a considerable range the size and diffusion parameters approximately offset each other so that collisional frequencies remain constant. The use of initial rates also minimized difficulties arising from the angular dependence of molecular weights estimated from light scattering intensity. Angular dependence of the apparent molecular weight of monomeric vesicles is minimal (Wei et al., 1982) but would be significant for the final aggregate.

Results

Measurement of Vesicle Aggregation Rates by Stopped-Flow Light Scattering. The addition of myelin basic protein to phospholipid vesicles caused a large, time-dependent increase in light scattering intensity due to vesicle aggregation (Figure 1). Aggregation rates were estimated from the initial, linear increase in light scattering intensity (Figure 1, inset A). Double logrithmic plots of initial rates vs. the concentration of phospholipid yielded lines of slope 2 (Figure 1, inset B). Therefore, the aggregation reaction was second order in phospholipid. Rate constants for the aggregation process were obtained by division of the initial slope by the molar concentration and initial scattering intensity of the vesicles (see Materials and Methods). Vesicles within the aggregates did not undergo fusion. This was shown by trypsin digestion of the protein in the complex which returned the vesicles to their original light scattering intensity and diffusion coefficient (Lampe & Nelsestuen, 1982). In the same study we documented conditions that allow membrane fusion in myelin basic protein aggregates.

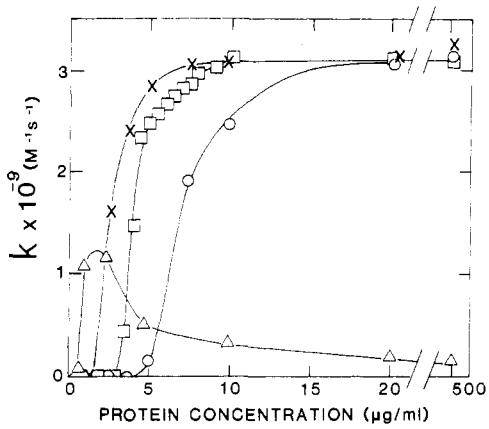

FIGURE 2: Effects of myelin basic protein (×, □, ○) and poly(L-lysine) (△) concentration on the observed rate constant for aggregation of PG/PC (30/70) vesicles. The concentrations of the vesicles (M_r 4.2 × 10^6) were (×) 3.0 × 10^{-9} M, (□) 6.0 × 10^{-9} M, (○) 1.20 × 10^{-8} M, and (△) 6.0 × 10^{-9} M.

Figure 2 shows the rate constants for aggregation of PG/PC (30/70) vesicles by myelin basic protein and poly(L-lysine). Poly(L-lysine) has been reported to cause multilayer membrane formation (Brady et al., 1981) and to aggregate vesicles (Lampe & Nelsestuen, 1982; Stollery & Vail, 1977). Poly(L-lysine) contains a 7× higher charge density (weight basis) than myelin basic protein and aggregated vesicles at lower peptide concentrations (Figure 2). However, on any basis of comparison, certain differences exist between myelin basic protein and poly(L-lysine)-mediated vesicle aggregation. Initial rates of vesicle aggregation by poly(L-lysine) showed characteristics expected for vesicle aggregation by peptide monomers; the rate constant reached a maximum and then decreased at higher peptide concentrations where the vesicles would be coated with protein monomers.

Myelin basic protein dependent vesicle aggregation rates showed several interesting features (Figure 2). The rate of aggregation was saturable with respect to protein but was not inhibited by the highest protein concentrations used here. The high affinity of protein for phospholipid indicated that complete saturation of the membrane surface was easily obtained in this concentration range. These observations indicated that myelin basic protein, unlike poly(L-lysine), cross-linked the vesicles through protein–protein interactions. Results for vesicles of 15 and 100% PG gave similar conclusions. Therefore, the protein monomer did not cross-link by binding the PG-rich areas on one vesicle and PC-rich areas on another. Ultimately, free protein monomers should bind to the membrane-bound protein and block aggregation. The available data on the interaction of monomeric protein (Smith, 1980, 1982) suggest that this will require much higher protein concentrations than were used in this study.

The protein dependence of aggregation was highly cooperative with a nearly stepwise approach to the maximum rate constant (Figure 2). The protein titration curve shifted with phospholipid concentration in a manner indicating that nearly all of the added protein was bound to the vesicles. If it is assumed that the half-maximal rate constant occurred at the same density of protein on the vesicles for all three vesicle concentrations, the shift in the total protein needed to generate the half-maximal rate constants could be used to estimate a free protein concentration of 3 × 10^{-8} M. Since initial rates of aggregation were used to construct the curves, and if it is assumed that protein–membrane binding had reached true equilibrium before significant aggregation occurred (see below), this value could be closely related to the dissociation

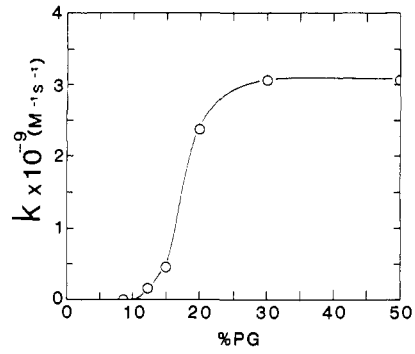

FIGURE 3: Effects of the percentage of PG in the vesicles on the rate constant at saturating protein concentration. Vesicles were prepared from the PG compositions given with PC added to total 100 mol %. Although initial aggregation rates were obtained at different protein concentrations, only those at saturating protein are plotted.

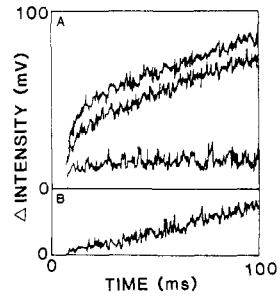

FIGURE 4: Chart tracing of fluorescence intensity when myelin basic protein and vesicles were mixed. The final concentration of the vesicles was 50 μg/mL. Part A: Vesicles were PG/dansyl-PE/PC (30/10/60). Protein concentrations were 40 μg/mL (upper curve), 10 μg/mL (middle curve), and 5 μg/mL (lower curve). Part B: Vesicles were PG/PC (30/70) and protein concentration was 20 μg/mL. Before each experiment, buffer and vesicles were mixed (i.e., no protein was added), and the resulting value was assigned a value of zero intensity.

constant for a simple protein–membrane complex. This value probably represents an upper limit for the protein–membrane dissociation constant.

The density of protein on the vesicle was also varied by restricting the density of PG. The initial rate constants obtained for different vesicle compositions at saturating protein levels are shown in Figure 3. The degree of cooperativity was similar to that shown in Figure 2. This result, obtained at saturating protein concentrations, demonstrated that the high degree of cooperativity was a function of the density of protein on the membrane rather than the rate of protein binding to the membrane. Vesicles of 30, 50, and 100% PG gave similar maximum rate constants, indicating that saturation with respect to PG and therefore protein density on the membrane had been reached.

An Arrhenius plot for the aggregation of PG/PC (30/70) vesicles at saturating protein concentration yielded an activation energy of 4.8 kcal/mol (n = 16, r = −0.95, data not shown). This value is near that expected for a diffusion-controlled reaction in water.

Protein–Membrane Binding Rates by Stopped-Flow Fluorescence Intensity. Experimental conditions were selected to measure fluorescence energy transfer from the tryptophan moiety in myelin basic protein to vesicle-bound dansyl-PE. This could occur when intermolecular distances are reduced by protein–membrane binding. A biphasic increase in light intensity was observed after mixing the protein and vesicles; a rapid increase was followed by an almost linear rise in light intensity (Figure 4A). Addition of protein to vesicles at a ratio where initial rates of aggregation were minimal (e.g., 5

Table I: Myelin Basic Protein–Membrane Fluorescence Intensity Changes and Reaction Half-Times

vesicle[a] concn (μg/mL)	protein concn (μg/mL)	ΔI[b] (mV)	$t_{1/2}$[c] (ms)
50	5	13	10
50	10	28	8
50	20	35	<8
50	40	40	<8
25	2.5	10	12
25	5	16	9
25	10	21	8
25	20	21	<8

[a] Vesicle composition was PG/dansyl-PE/PC (30/10/60). [b] Estimated by extrapolation of the linear secondary rise in light scattering to zero time (see Figure 4). [c] The first reaction half-time assuming a constant instrument dead time of 8 ms.

μg of vesicles; Figure 2) did not produce the secondary linear increase in light intensity (Figure 4A, lower curve). On the other hand, vesicles that contained no dansyl-PE and therefore could not participate significantly in fluorescence energy transfer displayed only the secondary linear rise (Figure 4B). These characteristics, along with the observation that the secondary increase in light intensity followed the general kinetics of aggregation, indicated that the secondary increase resulted from scattered light associated with vesicle aggregation. A small amount of polychromatic light passed by the excitation and/or emission filters would allow this to occur. The slow secondary rise in light intensity was therefore subtracted below analysis of protein–membrane binding.

The rapid increase in light intensity resulted primarily from fluorescence energy transfer from tryptophan to the dansyl moiety. Static fluorescence experiments run at protein:vesicle ratios where aggregation was minimal showed that the protein-induced increase in intensity at 510 nm occurred with excitation at 280 nm but not with direct excitation of the dansyl moiety at 350 nm. Therefore, the observed intensity changes did not result from increases in the dansyl quantum yield. Reaction half-times and relative intensity changes were obtained and are presented in Table I. The following observations indicated that the measurements represented protein–membrane binding: the change in intensity was saturable with respect to protein; the reaction half-time decreased with increasing protein; the intensity change at saturating protein was approximately proportional to the concentration of phospholipid.

Secondary Protein–Vesicle Aggregation. Although most of this study involved the use of initial rate data, additional information was obtained by studying the secondary association processes that occurred during aggregation. As shown elsewhere (Lampe & Nelsestuen, 1982), trypsin digestion caused complete dissociation of the aggregates to monomeric vesicles. Dissociation was also tested by dilution of aggregates with excess vesicles to produce a protein:phospholipid ratio that was less than that necessary for aggregation (see Figure 2). Under these circumstances, dissociation should occur if it were a simple reversal of the primary association we observed in the stopped-flow apparatus. Experimentally, only a slight decrease in the light scattering intensity occurred after mixing (data not shown). Therefore, the multimeric aggregates appear to be quite stable. This result would be expected for a three-dimensional lattice of cross-linked vesicles.

Under certain circumstances the time course of the light scattering intensity due to aggregation was sigmoidal (Figure 5). The length of the delay before the onset of aggregation depended on vesicle and protein concentrations and on the

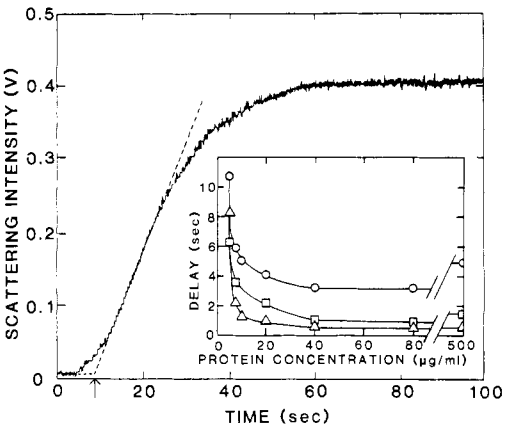

FIGURE 5: Chart tracing of the light scattering intensity when myelin basic protein and PG/PC (10/90) vesicles were mixed. Final concentrations were 5 μg of protein/mL and 25 μg of phospholipid/mL. The time from 0 to the arrow is defined as the delay (see the text). Inset: Effects of protein concentration on the delay. Vesicle compositions expressed as PG/PC ratios were (○) 8/92, (□) 10/90, and (△) 12/88.

percentage of acidic phospholipid in the vesicles. When PG/PC ratios greater than 20/80 were used, no delay in the onset of aggregation was observed when protein levels were at or near saturating (e.g., Figure 1). Dependence of the delay on protein is illustrated in Figure 5 (inset). At low PG/PC ratios, the delay was not eliminated by high protein concentrations, and the rate-determining event was therefore not related to a protein–membrane collision process. Low protein density on the vesicle was somehow responsible for the delay in aggregation. In these cases vesicle aggregation required a secondary process that involved an induction period.

Discussion

The goal of this study was to measure the initial rates of simple associations between myelin basic protein and phospholipid vesicles. The results at high protein densities indicated that formation of an aggregate involved a two-stage process consisting of protein–vesicle interaction followed by vesicle aggregation:

$$iP + V \overset{k_1}{\rightleftharpoons} (P_iV) \overset{k_2}{\rightleftharpoons} (P_iV)_n \qquad (1)$$

where P is protein, V is phospholipid vesicle, and $(P_iV)_n$ is the initial aggregated product. At low protein density a delay in the onset of aggregation was observed. The basis for the delay is unknown, but it appears to involve step 2 rather than step 1. One possible explanation is that at low protein density a vesicle dimer may have insufficient cross-linking for stability. A larger aggregate (trimer, tetramer, etc.) having multiple associations with different adjacent vesicles could form a stable network with fewer cross-links between any two vesicles. Formation of such an aggregate would have a lower probability so that an apparent delay in the onset of vesicle aggregation would be observed (e.g., Figure 5). Other explanations for the delay are also possible. The delay emphasizes the difference between initial rates of aggregation and final thermodynamic equilibrium; given adequate time aggregates form from a very broad ratio of protein or peptide to vesicles.

Initial velocity measurements were used here to obtain information about the properties of the simple protein–membrane interactions (i.e., steps 1 and 2 of eq 1). Stopped-flow fluorescence studies directly showed that protein binding to the vesicles was saturable with respect to protein and occurred faster than vesicle aggregation. The theoretical maximum rate constant for protein–vesicle collision (1.3×10^{10} M^{-1} s^{-1}) was

calculated by the Smoluchowski theory (1915, 1917) using the published diffusion coefficient (7.4×10^{-7} cm^2/s) and Stokes radius (2.9×10^{-7} cm, calculated from the Einstein–Sutherland equations) for myelin basic protein (Liebes et al., 1975) and the experimentally determined values for the vesicles (see below). This value was compared to an experimental rate constant calculated from half-times of myelin basic protein–membrane binding (Table I). The calculation was similar to that used in other studies (Wei et al., 1982; Pusey et al., 1982) and assumed a simple bimolecular interaction with independent noninteracting membrane-bound protein and a negligible dissociation rate. These assumptions are not unreasonable, and all were shown to be valid (Pusey et al., 1982) or nearly valid (Wei et al., 1982) for other extrinsic membrane-binding proteins. The maximum number of myelin basic protein molecules bound was calculated by using a ratio of 27 PG molecules per bound protein (Boggs et al., 1977, 1981). The reaction half-time of 8 ms (Table I) obtained at a protein concentration of 10 μg/mL and vesicle concentration of 50 μg/mL (PG/PC = 30/70) corresponded to a rate constant of 2×10^8 M^{-1} s^{-1}. A significant dissociation rate would increase this value. Since this calculation is expressed per protein molecule bound, it must be multiplied by the maximum number of proteins bound per vesicle (46) in order to compare it to the theoretical collisional rate constant between protein and vesicles (Wei et al., 1982). The rate constant per vesicle then became about 1×10^{10} M^{-1} s^{-1}. While this represents an approximation, the result is nearly equal to the theoretical collisional rate constant, and we conclude that the collisional efficiency for protein–membrane binding is high. This observation was consistent with our results for other extrinsic membrane-binding proteins under optimal conditions (Wei et al., 1982; Pusey et al., 1982).

The theoretical maximum rate constant for vesicle collision (6.6×10^9 M^{-1} s^{-1}) was calculated by using the diffusion constant (1.26×10^{-7} cm^2/s) and Stokes radius (1.7×10^{-6} cm) of the vesicles. The experimentally measured rate constant (3×10^9 M^{-1} s^{-1}, Figure 2) was about half of this value. Under optimal conditions it therefore appeared that both steps 1 and 2 (eq 1) were facile interactions requiring little molecular fitting.

The stopped-flow light scattering data supported several other conclusions regarding the nature of protein cross-linking of the vesicles. For example, the vesicle cross-links appeared to be due to protein–protein interactions so that the protein bridges the membrane as a dimer. This conclusion was derived primarily from the observation that the highest myelin basic protein concentrations did not inhibit vesicle aggregation rates although they should easily saturate the surface of the vesicles. This view is consistent with some previous results that have shown that bifunctional reagents cross-link myelin basic protein as a dimer in myelin (Golds & Braun, 1978a) and free in solution (Golds & Braun, 1978b). A study of the protein in solution indicated that the protein–protein interaction may be hydrophobic in nature and involve residues 81–118 (Chapman & Moore, 1976). Therefore, vesicle aggregation and possibly cross-linking of myelin lamellae may result from hydrophobic interactions between protein molecules.

The kinetics of myelin basic protein dependent cross-linking of membranes containing acidic phospholipids were highly cooperative with respect to membrane-bound protein. This was apparent whether protein density on the membrane was restricted by limiting the total protein (Figure 2) or by reducing the ability of the membrane to bind protein (Figure 3). Linear extrapolation of the association rate constant data to zero (Figure 2) indicated a molar ratio of about 20 myelin basic protein molecules per vesicle at all three vesicle concentrations. Since very little of the protein appeared to be free in solution under these circumstances, this number should closely represent the protein density on the membrane needed to obtain a measurable aggregation rate. A molar ratio of 18 was obtained from similar extrapolation of the data in Figure 3. This latter number was calculated from the density of PG in the membrane, from the reported number of PG molecules necessary to bind one protein molecule [27 (Boggs et al., 1977, 1981)], and with the assumption that 67% of the phospholipid is on the exterior of a vesicle. Conversely, these extrapolations to the minimum detectable rate constant could be used to calculate the number of PG molecules per bound myelin basic protein. The results would indicate a ratio of about 24 PG molecules per bound protein and thereby closely corroborate the ratios calculated by Boggs et al. (1977, 1981). The maximum vesicle association rate was attained at a ratio of about 35 protein molecules per vesicle (Figure 2).

Dimerization of myelin basic protein occurs with low affinity (Smith, 1982). Nevertheless, several weak protein–protein interactions could additively produce high affinity between vesicles and cause aggregation. This view is consistent with the highly cooperative protein dependence of vesicle aggregation (Figure 2). A low protein–protein affinity could also explain why the range of protein concentration did not inhibit vesicle aggregation. The latter should occur when protein monomers bind to vesicle-bound protein and block cross-linking. In another study, concentrations greater than 8 mg of protein/mL appeared necessary to inhibit vesicle aggregation (Smith, 1977b).

The several lines of evidence obtained here support the concept of vesicle cross-linking through multiple and therefore cooperative protein–protein interactions. Individual protein–protein associations are weak but collectively can form a very stable structure. This reasoning should also apply to myelin, which has a high density of this protein (Rumsby & Crang, 1977).

Registry No. Poly(L-lysine), 25104-18-1; poly(L-lysine), SRU, 38000-06-5.

References

Boggs, J. M., & Moscarello, M. A. (1978a) *Biochim. Biophys. Acta 515*, 1–21.

Boggs, J. M., & Moscarello, M. A. (1978b) *J. Membr. Biol. 39*, 75–96.

Boggs, J. M., Moscarello, M. A., & Papahadjopoulos, D. (1977) *Biochemistry 16*, 5420–5426.

Boggs, J. M., Wood, D. D., & Moscarello, M. A. (1981) *Biochemistry 20*, 1065–1073.

Brady, G. W., Murthy, N. S., Fein, D. B., Wood, D. D., & Moscarello, M. A. (1981) *Biophys. J. 34*, 345–350.

Chapman, B. E., & Moore, W. J. (1976) *Biochem. Biophys. Res. Commun. 73*, 758–766.

Chen, P. S., Toribara, T. Y., & Warner, H. (1956) *Anal. Chem. 28*, 1756–1758.

Epand, R. M., Moscarello, M. A., Zierenberg, B., & Vail, W. J. (1974) *Biochemistry 13*, 1264–1267.

Eylar, E. H., Kniskern, P. J., & Jackson, J. J. (1974) *Methods Enzymol. 32B*, 323–341.

Golds, E. E., & Braun, P. E. (1976) *J. Biol. Chem. 251*, 4729–4735.

Golds, E. E., & Braun, P. E. (1978a) *J. Biol. Chem. 253*, 8165–8170.

Golds, E. E., & Braun, P. E. (1978b) *J. Biol. Chem. 253*, 8171–8177.

Hax, W. M. A., & Geurts Van Kessel, W. S. M. (1977) *J. Chromatogr. 142*, 735–741.
Jones, A. J. S., & Rumsby, M. G. (1977) *Biochem. J. 167*, 583–591.
Kremer, J. M. H., Esker, M. W. J., Pathmamanoharan, C., & Wiersema, P. H. (1977) *Biochemistry 16*, 3932–3935.
Lampe, P. D., & Nelsestuen, G. L. (1982) *Biochim. Biophys. Acta 693*, 320–325.
Liebes, L. F., Zand, R., & Phillips, W. D. (1975) *Biochim. Biophys. Acta 405*, 27–39.
London, Y., Demel, R. A., Guerts Van Kessel, W. S. M., Vossenberg, F. G. A., & Van Deenen, L. L. M. (1973) *Biochim. Biophys. Acta 311*, 520–530.
Peterson, R. G., & Gruener, R. W. (1978) *Brain Res. 152*, 17–28.
Pletcher, C. H., Resnick, R. M., Wei, G. J., Bloomfield, V. A., & Nelsestuen, G. L. (1980) *J. Biol. Chem. 255*, 7433–7438.
Poduslo, J. F., & Braun, P. E. (1975) *J. Biol. Chem. 250*, 1099–1105.
Pusey, M. L., Mayer, L. D., Wei, J. G., Bloomfield, V. A., & Nelsestuen, G. L. (1982) *Biochemistry 21*, 5262–5269.
Rumsby, M. G., & Crang, A. J. (1977) *Cell Surf. Rev. 4*, 247–362.
Smoluchowski, M. (1915) *Ann. Phys. (Liepzig) 48*, 1103.
Smoluchowski, M. (1917) *Z. Phys Chem., Stoechiom. Verwandtschaftsl. 92*, 129.
Smith, R. (1977a) *Adv. Exp. Med. Biol. 100*, 221–234.
Smith, R. (1977b) *Biochim. Biophys. Acta 470*, 170–184.
Smith, R. (1980) *Biochemistry 19*, 1826–1831.
Smith, R. (1982) *Biochemistry 21*, 2697–2701.
Smith, R., & McDonald, B. J. (1979) *Biochim. Biophys. Acta 554*, 133–147.
Stollery, J. G., & Vail, W. J. (1977) *Biochim. Biophys. Acta 471*, 372–390.
Stollery, J. G., Boggs, J. M., Moscarello, M. A., & Deber, C. M. (1980) *Biochemistry 19*, 2391–2396.
Waggoner, A. S., & Stryer, L. (1970) *Proc. Natl. Acad. Sci. U.S.A. 67*, 579–589.
Weber, K., & Osborn, M. (1969) *J. Biol. Chem. 244*, 4406–4412.
Wei, G. J., Bloomfield, V. A., Resnick, R. M., & Nelsestuen, G. L. (1982) *Biochemistry 21*, 1949–1959.

Absence of Pyridoxine- (Pyridoxamine-) 5′-phosphate Oxidase in Morris Hepatoma 7777†

Louise M. Nutter,‡ Natalie T. Meisler, and John W. Thanassi*

ABSTRACT: Morris hepatoma 7777 previously has been shown to have no detectable pyridoxine- (pyridoxamine-) 5′-phosphate oxidase activity [Thanassi, J. W., Nutter, L. M., Meisler, N. T., Commers, P., & Chiu, J.-F. (1981) *J. Biol. Chem. 256*, 3370–3375]. In order to determine if this enzyme was missing in the hepatoma, we purified rat liver oxidase and raised antibodies to it in rabbits. Final purification of rat liver oxidase for use as an antigen was accomplished by affinity chromatography and gel electrophoresis. The rat liver enzyme is similar to rabbit liver oxidase [Kazarinoff, M. N., & McCormick, D. B. (1975) *J. Biol. Chem. 250*, 3436–3442] having two noncovalently linked subunits with molecular weights in the range of 25 000–28 000. Evidence indicating that inactive enzyme was simultaneously purified with native enzyme was obtained. The IgG fraction was purified from the serum of a rabbit that had been immunized with rat liver oxidase. This was used in the development of ELISA and immunoblot analyses for the presence of antigenically active pyridoxine- (pyridoxamine-) 5′-phosphate oxidase in cytosolic preparations from normal rat liver and Morris hepatoma 7777. The results indicated that there was no immunologically detectable oxidase protein in the tumor. An alternate pathway of pyridoxal 5′-phosphate synthesis, involving oxidation of pyridoxine to pyridoxal followed by phosphorylation, was ruled out. The implications of these findings with respect to acquisition of nutrients by tumors are discussed.

Pyridoxine- (pyridoxamine-) 5′-phosphate oxidase (EC 1.4.3.5) is responsible for the formation of pyridoxal 5′-phosphate, the coenzymatically active form of vitamin B-6, from phosphorylated precursor forms (Wada & Snell, 1961). This enzyme has been purified from rabbit liver (Kazarinoff & McCormick, 1975), pig brain (Kwok & Churchich, 1980), rat brain (Cash et al., 1980), and bakers' yeast (Tsuge et al., 1979). It has been extensively studied by McCormick and co-workers (Merrill et al., 1979; McCormick & Merrill, 1980; Tsuge & McCormick, 1980; Choi & McCormick, 1981), who have proposed that it plays a regulatory role in vitamin B-6 metabolism (Merrill et al., 1978). Homogeneous oxidase preparations obtained from rabbit liver (Kazarinoff & McCormick, 1975) and pig brain (Kwok & Churchich, 1980) are reported to have molecular weights of 54 000 and 60 000, respectively, and contain one tightly bound FMN per active monomer which is composed of two noncovalently linked subunits.

We have previously found that two poorly differentiated Morris hepatomas lack pyridoxine- (pyridoxamine-) 5′-phosphate oxidase activity (Thanassi et al., 1981). In addition, we have reported that there appears to be an oncodevelop-

† From the Department of Biochemistry, University of Vermont, College of Medicine, Burlington, Vermont 05405. *Received September 8, 1982.* This research was supported by U.S. Public Health Service Grant AM 25490 and BRSG Grant 2-32908 from the University of Vermont College of Medicine. L.M.N. gratefully acknowledges support provided by a private gift to the University of Vermont.
‡ Cancer Biology Trainee supported by U.S. Public Health Service Grant CA T32-09826.

0006-2960/83/0422-1599$01.50/0